Electronic Supplementary Material (ESI) for Dalton Transactions.

The addition of bromine and iodine on palladacyclopentadienyl complexes bearing bidentate heteroditopic P−N spectator ligands derived from differently substituted quinolinic frames. The unexpected evolution of the reaction.

L. Canovese, *[a] F. Visentin, [a] T. Scattolin, [a] C. Santo [a] and V. Bertolasi [b]

[a] *Dipartimento di Scienze Molecolari e Nanosistemi, Università Ca' Foscari, Venice, Italy, and*

[b] *Dipartimento di Chimica e Centro di Strutturistica Diffrattometrica, Università di Ferrara, Ferrara, Italy.*

Table of contents

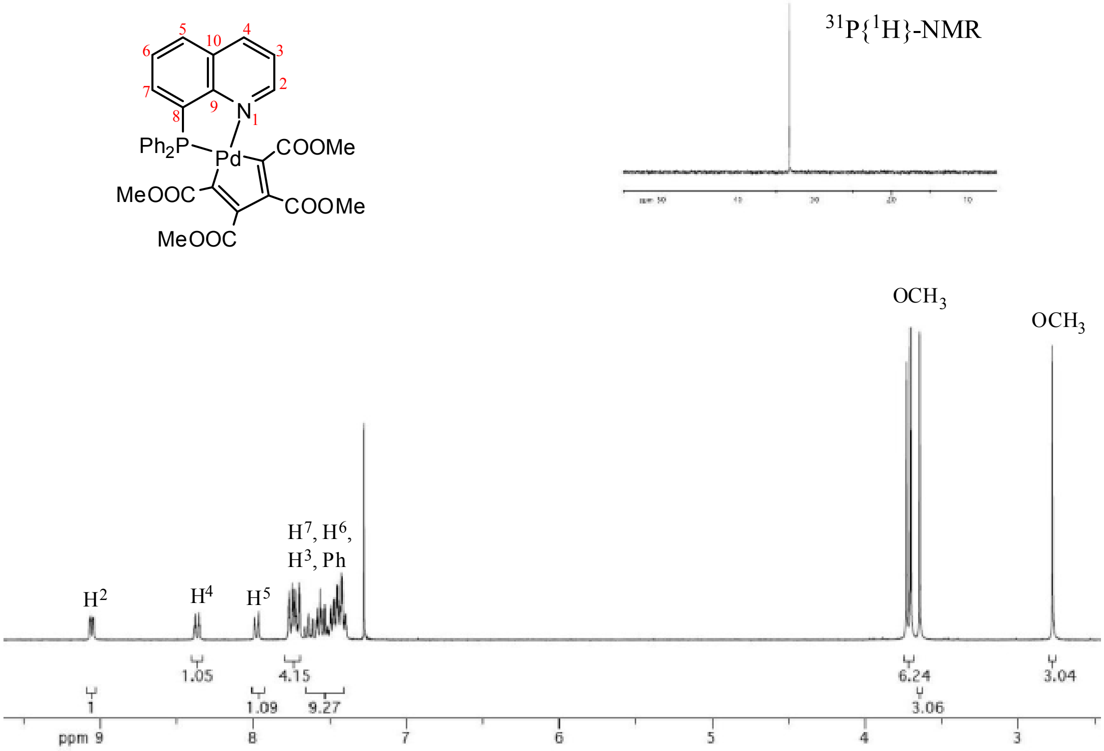

Fig 1SI. ^{1}H and ^{31}P NMR spectra of complex **1a** in $CDCl_3$ at 298 K.

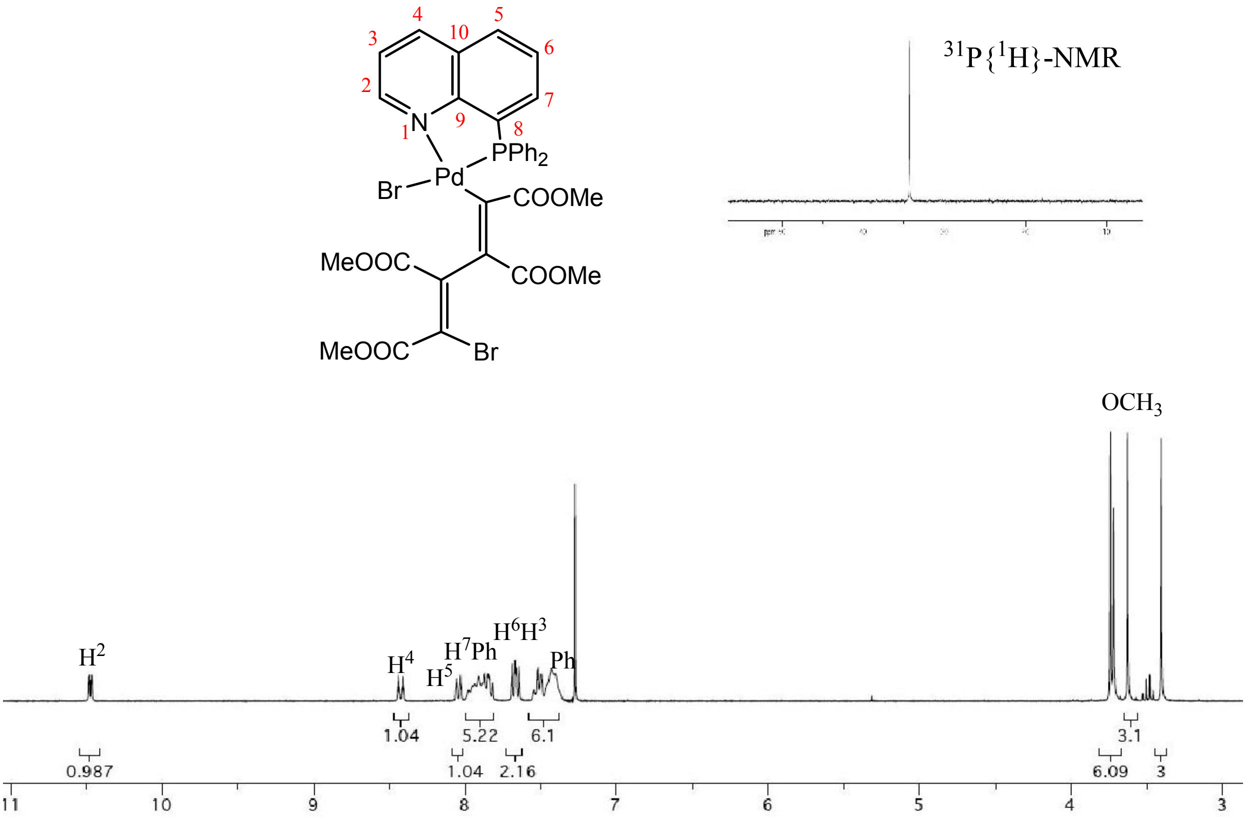

Fig 2SI. ^{1}H and ^{31}P NMR spectra of complex **2a** in $CDCl_3$ at 298 K.

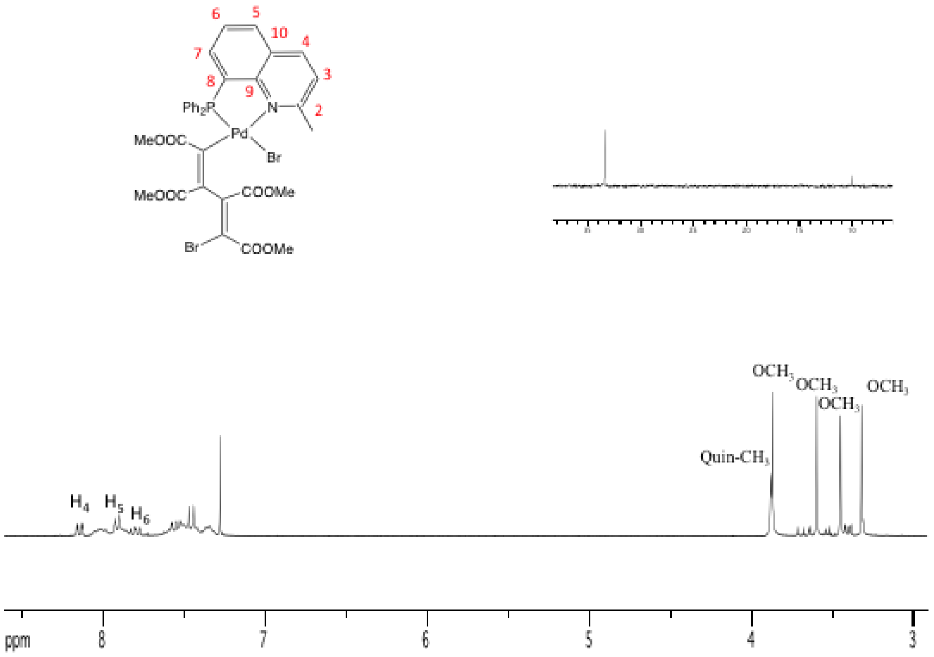

Fig 3SI. ^{1}H and ^{31}P NMR spectra of complex **2b** in $CDCl_3$ at 298 K.

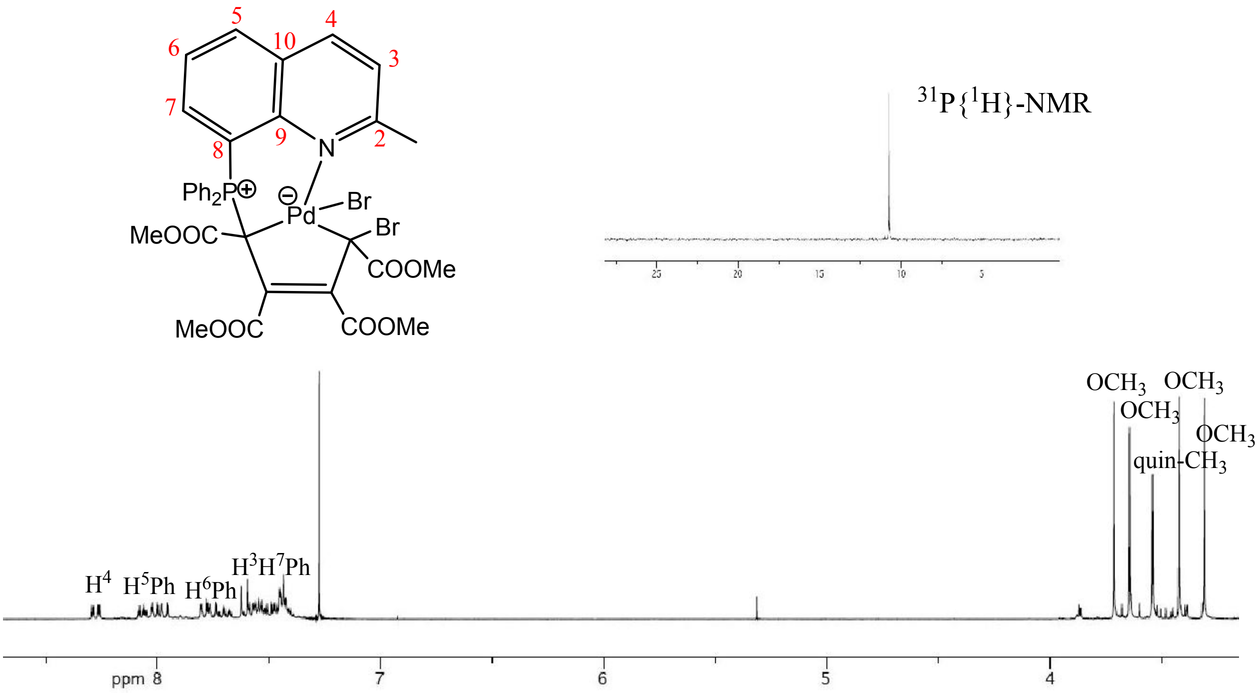

Fig 4SI. ^{1}H and ^{31}P NMR spectra of complex **4b** in $CDCl_3$ at 298 K.

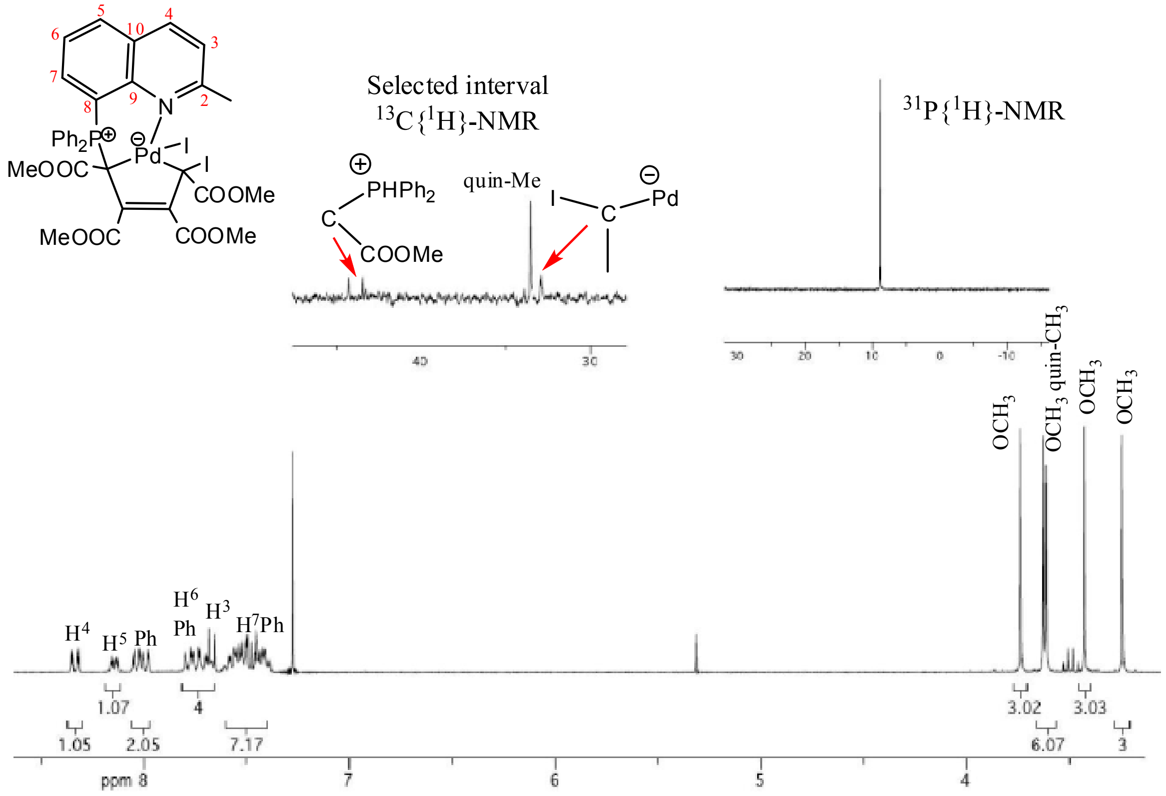

Fig 5SI. ^{1}H, ^{31}P and a selected section of ^{13}C NMR spectra of complex **5b** in $CDCl_3$ at 298 K.

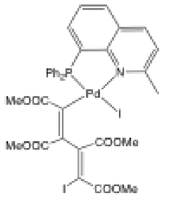

3b

*

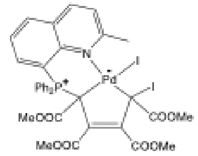

5b

0

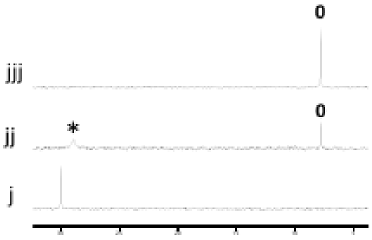

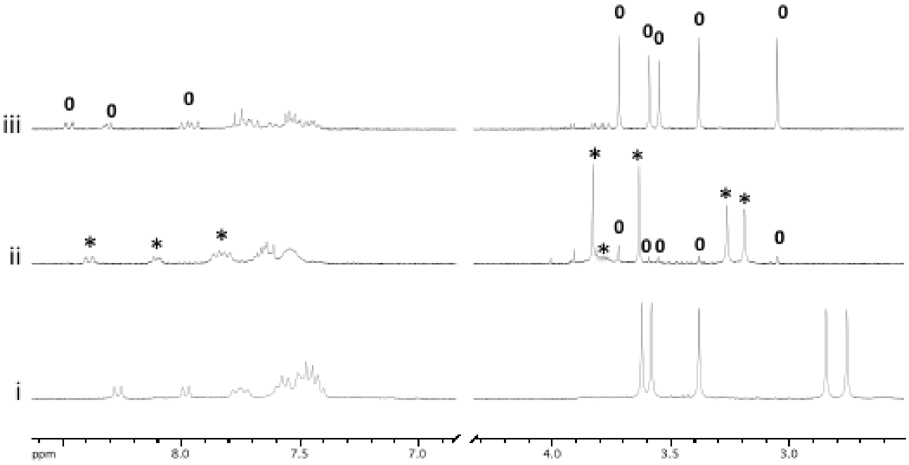

Fig. 6SI. ^1H, ^{31}P NMR spectra of reaction between complex **1b** and I_2. (*i*, *j*) t = 0; (*ii*, *jj*) some minutes after I_2 addition; (iii, jjj) final spectrum. $[\mathbf{1b}]_0 \approx 1.1 \times 10^{-2}$;; $[I_2]_0 \approx 2 \times 10^{-2}$ M, in CD_2Cl_2 at 253 K.

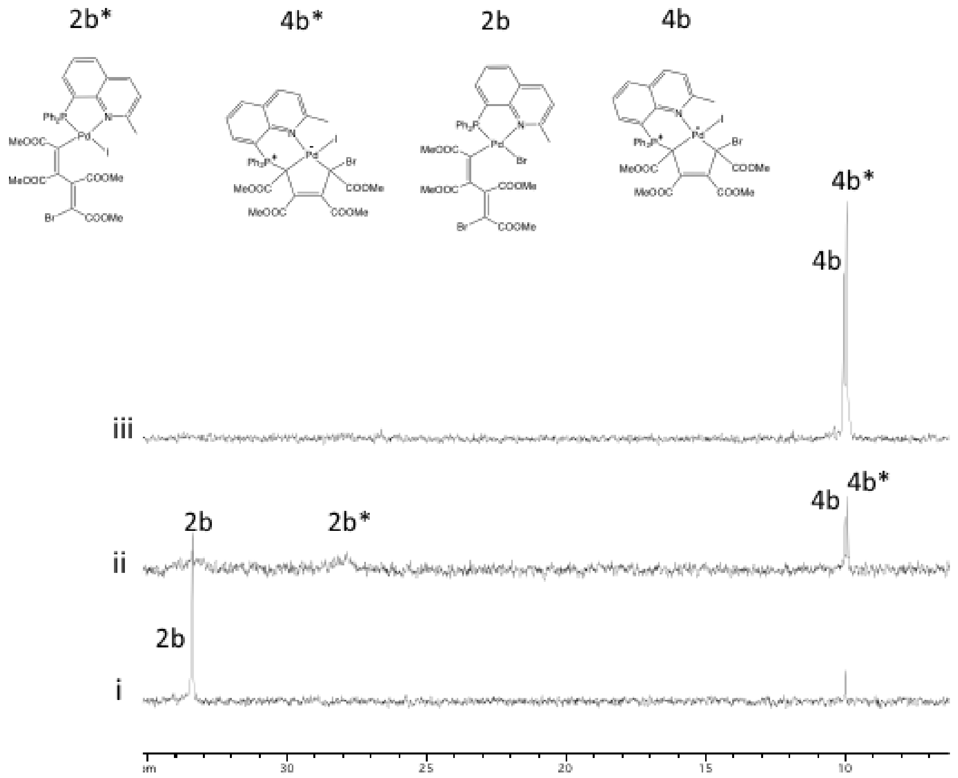

Fig. 7aSI. Selected ^{31}P NMR portion of the spectra of the reaction between **2b** and (*n*-Bu)$_4$NI. (i) t = 0, (ii); t =12' after the addition of (*n*-Bu)$_4$NI; (iii), t = 6h. [**2b**]$_0$ ≈ 1x10^{-2} M, [(*n*-Bu)$_4$NI)]$_0$ ≈ 2x10^{-2} M in CD$_2$Cl$_2$ at 298 K.

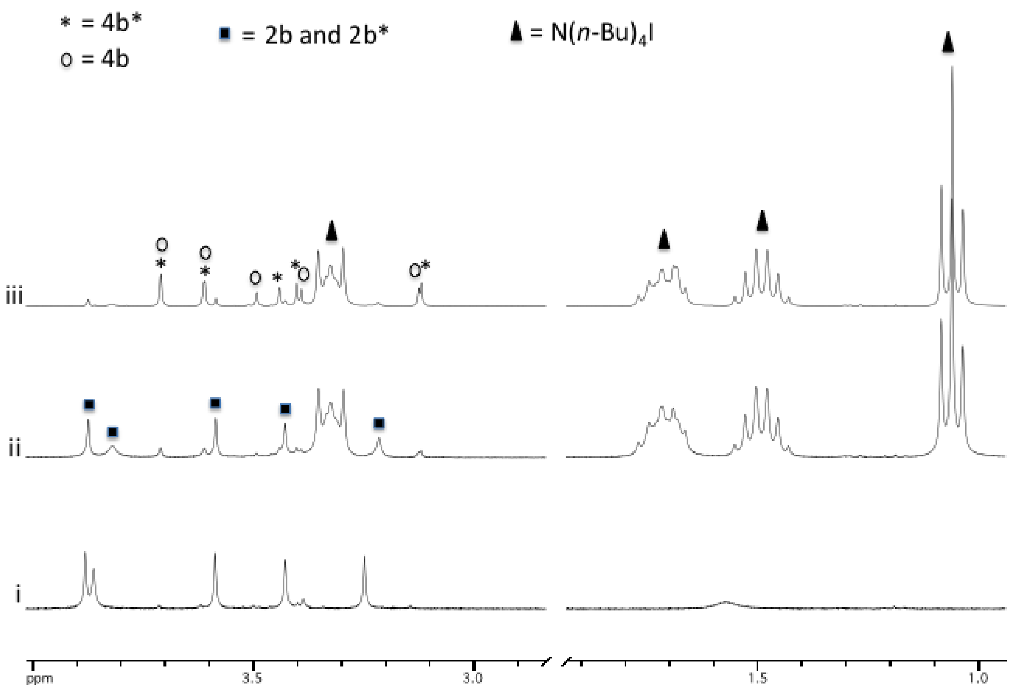

Fig. 7bSI. Selected ^{1}H NMR portion of the spectra of the reaction between **2b** and (n-Bu)$_4$NI. (i) t = 0, (ii); t =10' after the addition of (n-Bu)$_4$NI; (iii), t = 6h. [**2b**]$_0$ ≈ 1x10^{-2} M, [(n-Bu)$_4$NI)]$_0$ ≈ 2x10^{-2} M in CD$_2$Cl$_2$ at 298 K.

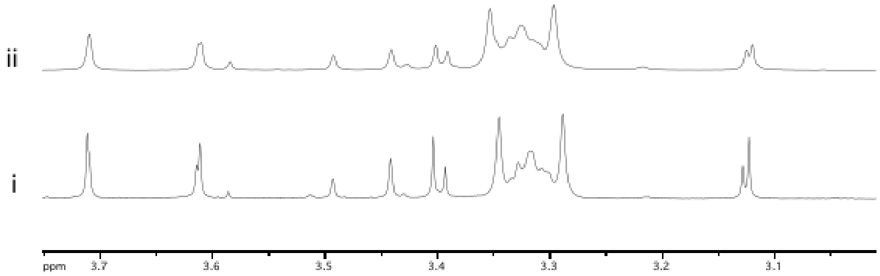

Fig. 7cSI. (i) Selected portion of ^{1}H NMR spectrum of the reaction between **4b** and (n-Bu)$_4$NI (t ≈ 10'). (ii) Selected portion of ^{1}H NMR spectrum of the reaction between **2b** and (n-Bu)$_4$NI t = 6h. $[\mathbf{4b}]_0 \approx 1\text{x}10^{-2}$, $[\mathbf{2b}]_0 \approx 1\text{x}10^{-2}$, $[(n\text{-Bu})_4\text{NI}]_0 \approx 2\text{x}10^{-2}$ M in CD_2Cl_2 at 298 K.

Schematic computational outcomes

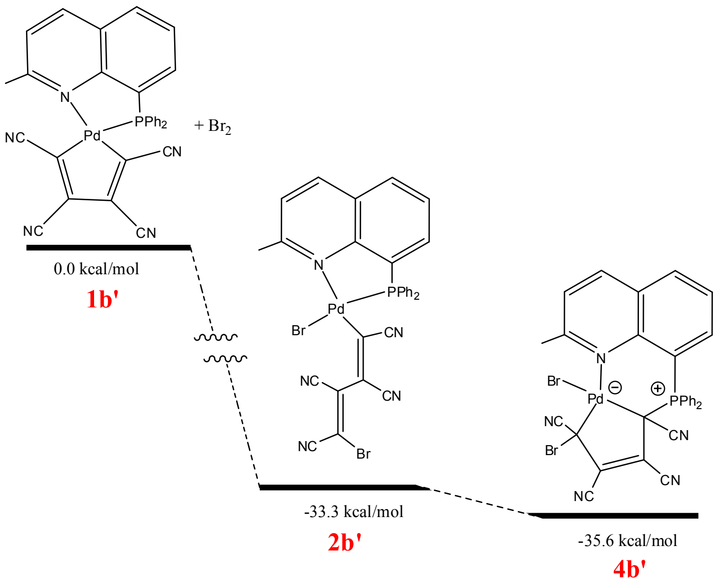

Fig 8aSI: Schematic computational outcomes for complexes **1b'**, **2b'**, **4b'**.

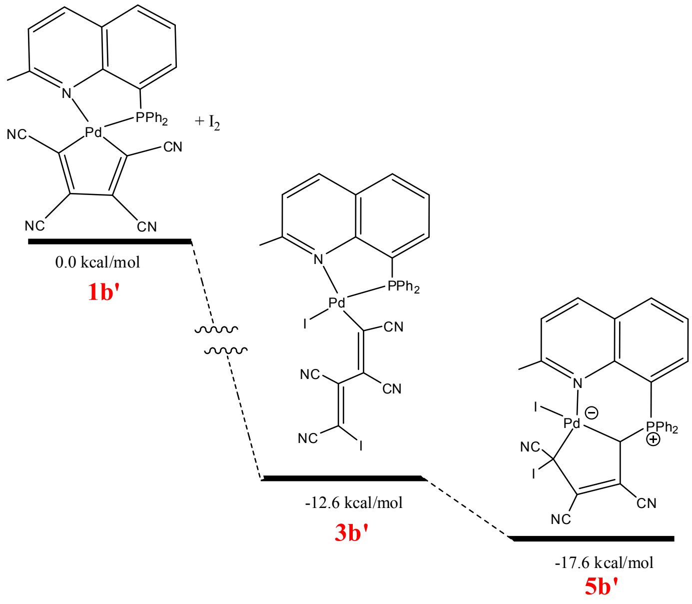

Fig 8bSI: Schematic computational outcomes for complexes **1b'**, **3b'**, **5b'**.

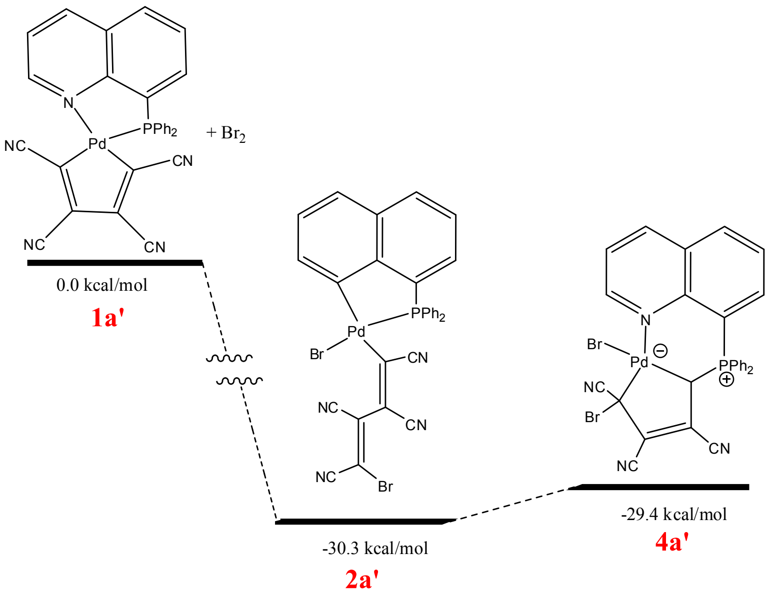

Fig 8cSI: Schematic computational outcomes for complexes **1a'**, **2a'**, **4a'**.

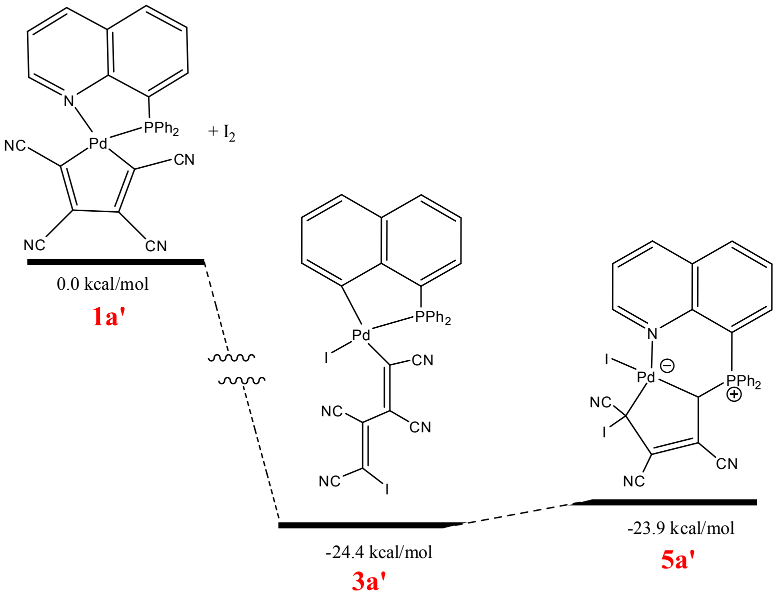

Fig 8dSI: Schematic computational outcomes for complexes **1a'**, **3a'**, **5a'**.

Complex	Pd-P bond length (Å)
2a'	2.2932 [a]
3a'	2.3113
2b'	2.2848
3b'	2.3017

Complex	Pd-C bond legth (Å)
4a'	2.1061
5a'	2.1202
4b'	2.0981 [b]
5b'	2.1117 [c]

Table 1SI. Calculated bond lengths for CN substituted complexes (see text).

[a] See Pd1-P1 Tab. 2SI (complex **2a**),

[b] see Pd1- C23 Tab. 2SI (complex **4b**),

[c] see Pd1-C23 Tab. 2SI complex (**5b**)

Distances (Å)	**2a**	**4b**	**5b**
Pd1-Br1	2.4995(4)	2.5008(4)	
Pd1-I1			2.6732(3)
Pd1-N1	2.139(3)	2.105(3)	2.097(2)
Pd1-P1	2.2370(8)		
Pd1-C22	2.008(3)		
Pd1-C23		2.103(3)	2.109(3)
Pd1-C26		2.035(3)	2.036(3)
P1-C23		1.817(3)	1.816(3)
C22-C23	1.339(4)		
C23-C24	1.489(4)	1.497(5)	1.500(4)

C24-C25	1.332(5)	1.333(5)	1.336(4)
C25-C26		1.501(4)	1.499(4)
Angles (°)			
Br1-Pd1-N1	94.00(7)	89.87(8)	
Br1-Pd1-P1	176.28(3)		
Br1-Pd1-C22	86.40(8)		
Br1-Pd1-C23		167.36(9)	
Br1-Pd1-C26		94.57(9)	
I1-Pd1-N1			88.99(7)
I1-Pd1-C23			164.82(8)
I1-Pd1-C26			95.95(9)
N1-Pd1-P1	84.15(7)		
N1-Pd1-C22	177.35(11)		
N1-Pd1-C23		92.70(12)	92.50(11)
N1-Pd1-C26		170.33(12)	171.28(11)
P1-Pd1-C22	95.31(9)		
C23-Pd1-C26		84.84(13)	84.62(12)
Pd1-C22-C23	127.0(2)		
Pd1-C23-C24		107.3(2)	107.4(2)
Pd1-C26-C25		108.9(5)	109.5(2)
C22-C23-C24	124.0(3)		
C23-C24-C25	122.1(3)	118.9(3)	118.8(3)
C24-C25-C26		118.9(3)	118.6(3)

Table 2SI. Selected bond distances and angles (Å and degrees) for compounds **2a, 4b** and **5b**.

Compound	**2a**	**4b**	**5b**
Formula	$C_{33}H_{28}Br_2NO_8PPd$	$C_{34}H_{30}Br_2NO_8PPd\cdot CH_2Cl_2$	$C_{34}H_{30}I_2NO_8PPd\cdot CH_2Cl_2$
M	863.73	962.69	1056.69
Space group	$P2_1/n$	$P2_1/n$	$P2_1/n$
Crystal system	Monoclinic	Monoclinic	Monoclinic
a/Å	13.9247(2)	11.7017(1)	11.8881(1)
b/Å	13.3155(2)	26.5544(3)	27.2222(3)
c/Å	18.1663(2)	12.1475(1)	12.0742(2)
β/°	96.4251(8)	100.5665(4)	100.7290(5)
U/$Å^3$	3347.14(8)	3710.61(6)	3839.15(8)
Z	4	4	4
T/K	295	295	295
D_c/g cm^{-3}	1.714	1.723	1.828
F(000)	1712	1912	2056
μ(Mo-Kα)/cm^{-1}	30.41	28.92	23.22
Measured Reflections	39432	40606	41928
Unique Reflections	9725	10748	11091
R_{int}	0.0746	0.0512	0.0663
Obs. Refl.ns [$I \geq 2\sigma(I)$]	7048	8281	6896
θ_{min}- θ_{max}/°	3.80 – 30.00	3.53 – 30.00	3.49 – 30.00
hkl ranges	-19,19;-18,16;-20,25	-16,16;-37,34; -17,14	-16,16;-38,38; -16,13
$R(F^2)$ (Obs.Refl.ns)	0.0409	0.0453	0.0371
$wR(F^2)$ (All Refl.ns)	0.1034	0.1247	0.0833
No. Variables	419	456	456

Goodness of fit	1.016	1.026	0.982
$\Delta\rho_{max}$; $\Delta\rho_{min}$ /e Å^{-3}	1.61; -1.26	1.14;-1.19	0.63;-0.75
CCDC Deposition N.	1053523	1053524	1053525

Table 3SI. Crystallographic data.

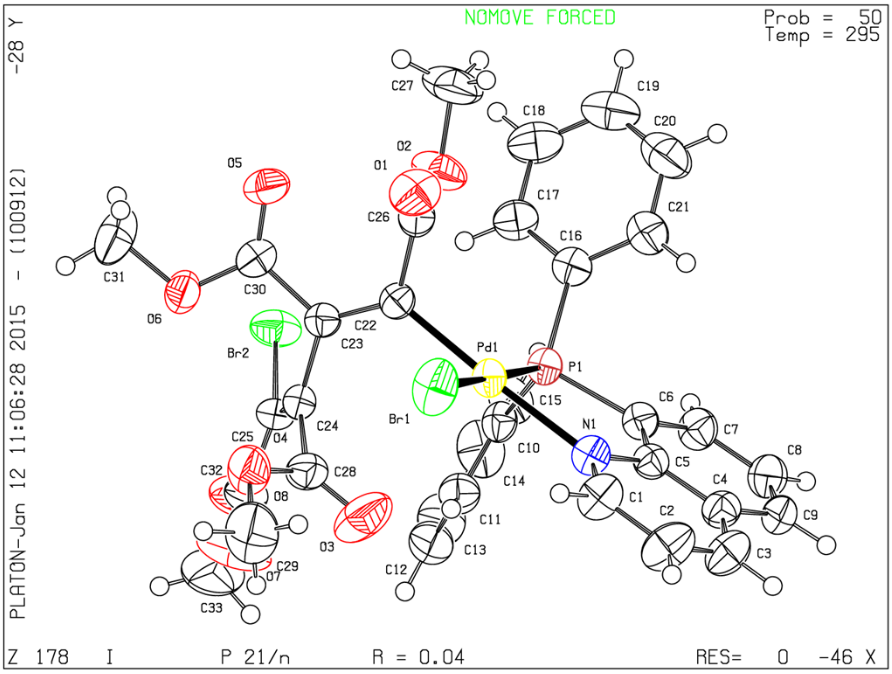

Fig 8SI. Ortep representation of complex **2a**

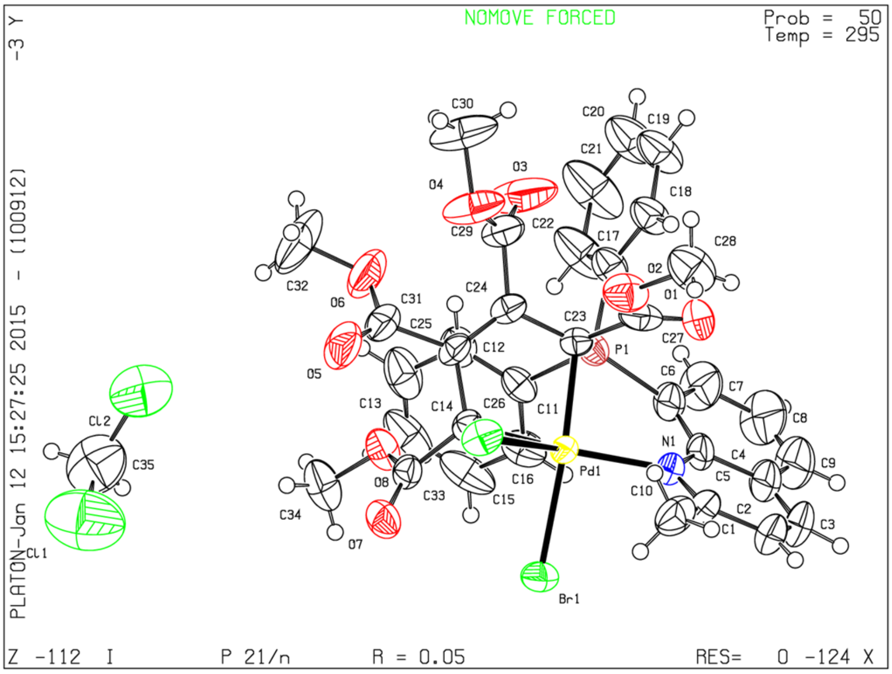

Fig 9SI. Ortep representation of complex **4b**

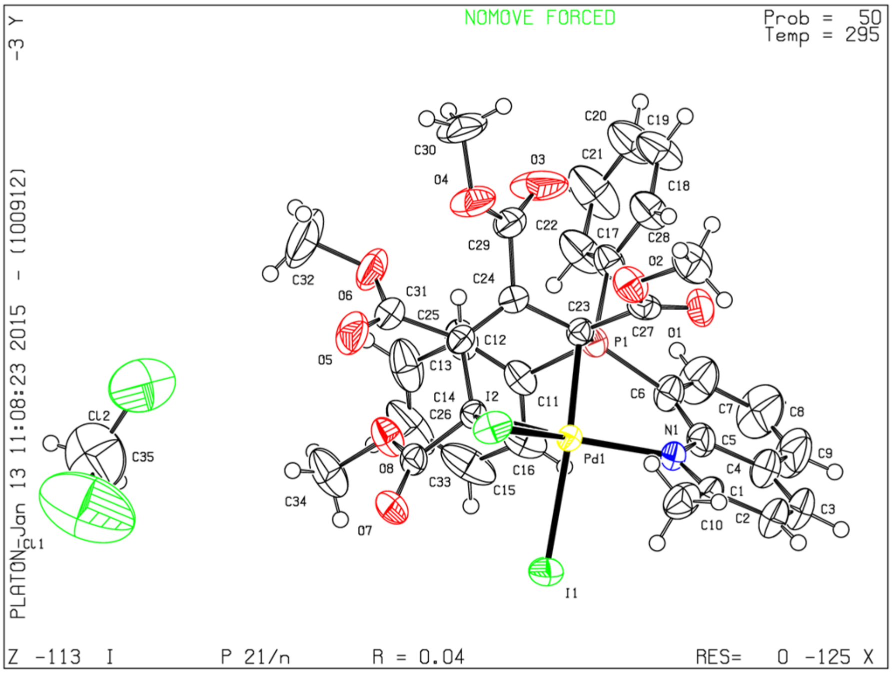

Fig 10SI. Ortep representation of complex **5b**

Footnote SI 1.

The observed process is a slow first order reaction, reaching smoothly an equilibrium mixture. This fact suggests an intramolecular conversion of **2b** into **4b,** instead of an intermolecular reaction which would be described by a second-order process.

We have determined the rate constants k_f and k_r ($k_f = 4.91 \times 10^{-5}$, $k_r = 9.1 \times 10^{-6}\ s^{-1}$) and the concentration at t = 0 of **2b** and **4b** ($[\mathbf{2b}]_0 = 8.8 \times 10^{-3}$, $[\mathbf{4b}]_0 = 1.16 \times 10^{-3}$ mol dm^{-3}) by parameter optimization of the solution of the differential equation system via non-linear regression:

$$\frac{d[2b]}{dt} = -k_f[2b] + k_r[4b]$$

$$\frac{d[4b]}{dt} = k_f[2b] - k_r[4b]$$

implemented in the SCIENTIST® computing environment.

An alternative approach would involve non linear regression of $[\mathbf{2b}]_t$ (or $[\mathbf{4b}]_t$) vs. t data to the model based on the analytical integration of the differential system:

$$[2b]_t = \frac{k_r}{k_e}\left([2b]_0 + [4b]_0\right) + \frac{\left(k_f[2b]_0 - k_r[4b]_0\right)}{k_e} e^{-k_e t}$$

Where $k_e = (k_f + k_r)$

However, the four parameters k_f, k_r, $[\mathbf{2b}]_0$, $[\mathbf{4b}]_0$ are extremely correlated even though their optimized values are almost coincident with those derived from the differential model